



Article

Experimental Investigation of Peening Cylindrical Workpieces Utilizing a Transducer with Ring Sonotrode

Fushi Bai ^{1,2,*} , Liang Wang ^{2,3}, Kunde Yang ¹, Zhengyao He ¹, Gang Qi ² and Jens Twiefel ² 

¹ School of Marine Science and Technology, Northwestern Polytechnical University, Xi'an 710072, China; ykdzym@nwpu.edu.cn (K.Y.); hezhengyao@nwpu.edu.cn (Z.H.)

² Institute of Dynamics and Vibration Research, Leibniz University Hannover, Appelstraße 11, 30167 Hannover, Germany; lwang@nuaa.edu.cn (L.W.); qigangalex890820@gmail.com (G.Q.); twiefel@ids.uni-hannover.de (J.T.)

³ State Key Laboratory of Mechanics and Control of Mechanical Structures, Nanjing University of Aeronautics and Astronautics, Yudao 29, Nanjing 210016, China

* Correspondence: baifushi@nwpu.edu.cn

Abstract: In industrial applications, the shafting components with high stress are easily damaged due to cyclic loads if there is no surface treatment. With the use of ultrasonic cavitation peening, the residual compressive stress and the surface hardness of these components can be improved. While traditional longitudinal vibration transducers are used to treat cylindrical workpieces, the treated areas are limited, and the treatment period is relatively long. To solve these problems, we designed a novel configuration of the piezoelectric transducer as a type of the combination of rod and ring. During ultrasonic cavitation peening, we placed the cylindrical workpieces in the ring tool to improve the limitation. However, the treated surface properties were largely influenced by the input parameters (driving voltage and rod diameters). In this investigation, the cylindrical workpieces, which were covered with aluminum foils, were first treated by ultrasonic cavitation peening to detect the intensity and distribution of the cavitation bubbles on the treated surface. Then, the sonochemiluminescence method was utilized as an additional way to find the optimal operation parameters (190 V and 16 mm). Finally, the ultrasonic cavitation process was conducted with the optimal parameters. The treatment results showed that the surface hardness increased by about 36% without significant increase of the surface roughness.

Keywords: ultrasonic cavitation; sonochemiluminescence; roughness; micro-hardness



Citation: Bai, F.; Wang, L.; Yang, K.; He, Z.; Qi, G.; Twiefel, J. Experimental Investigation of Peening Cylindrical Workpieces Utilizing a Transducer with Ring Sonotrode. *Appl. Sci.* **2021**, *11*, 94. <https://dx.doi.org/10.3390/app11010094>

Received: 19 November 2020

Accepted: 21 December 2020

Published: 24 December 2020

Publisher's Note: MDPI stays neutral with regard to jurisdictional claims in published maps and institutional affiliations.



Copyright: © 2020 by the authors. Licensee MDPI, Basel, Switzerland. This article is an open access article distributed under the terms and conditions of the Creative Commons Attribution (CC BY) license (<https://creativecommons.org/licenses/by/4.0/>).

1. Introduction

In modern industrial applications, cylindrical components, such as shafts, bearings, and screws, are widely used in aerospace, ship, marine, and automotive industries [1,2]. Due to the influence of high cycle fatigue and cyclic stress, these components have to retain a long service life to reduce the replacement frequency and cost. Therefore, a surface enhancement process is required after manufacturing. One of the often-used processes is the peening process, which is a physical method [3]. In the traditional method, sand pills and iron pills are typically used [4]. They are ejected with high speed and collide with the workpiece surfaces to improve the fatigue strength and change the surface properties of metal materials by generating surface compressive residual stresses. The traditional method is a simple way to treat the surfaces of metallic rods. Sakamoto [5] found that the cylindrical workpieces of annealed medium carbon steel were peened with 140–2300% coverage by the traditional process and that the fatigue limits increased 14–25% compared to the non-peened workpieces. However, the traditional peening process tends to increase the surface roughness, causing a certain damage and limiting the improvement of surface properties.

Ultrasonic needle peening is another method to peen cylindrical workpieces. An actuator is used to generate oscillation, which leads to a relative movement between the

sonotrode and the workpiece surface [6]. The sonotrode end is excited with a high frequency (more than 20 kHz) and directly impacts the workpiece surface. Utilizing this method topeen the cylindrical workpieces of Ti-6Al-4V, researchers showed in their experimental results that the 10^8 cycles fatigue strength can improve by 11.7% [7]. The compressive residual stress and the surface hardness increased as well. The solid steel pin is modeled as a rigid material [8]. The simulation results showed that the surface roughness magnitude depends on the correlation of the vertical and lateral load components. In this process, a rotated equipment is required for the rotation of the cylindrical specimen. Otherwise, the treating area is relatively small.

During water peening process, water cavitation jet goes through a peening nozzle with high speed [9]. When the bubbles are injected with a flow on a metal workpiece surface, a plastic deformation can be developed. Water cavitation jet peening utilizes this deformation. A Ti-6Al-4V rod with a diameter of 5 mm was investigated using this process and it was found that the depth of the introduced compressive residual stress increased up to 230 μm at a processing time per unit length of 10 s/mm [10]. The laser peening process uses high-energy pulsed laser to generate shock waves on the surfaces of the treated surfaces [11]. Yang et al. [12] investigated the effects of laser peening on residual stresses in 7050-T7451 aluminum alloy rods. The results showed that the geometrical effects of the curved target surface greatly influenced residual stress fields.

Compared to the traditional shot peening and ultrasonic needle peening, the mentioned shotless peening methods (water cavitation peening and laser peening) require skilled operators as well as expensive and complicated equipment. In order to achieve good surface properties with simple equipment, ultrasonic cavitation peening has been developed in recent decades [13–15]. During ultrasonic cavitation peening, a piezoelectric transducer is utilized and the sonotrode is partially immersed in a liquid. The results showed that the hardness and the residual compressive stress were significantly improved but the surface roughness was not obviously increased. Using a piezoelectric transducer has many advantages: simple equipment, compact structure, as well as a high output power [16]. Due to the vibration of the transducer sonotrode, cavitation bubbles are generated and then collapsed on the treated surfaces, which introduces the compressive residual stress and increases the surface hardness. When the ultrasonic cavitation peening is completed, the remaining material in water, such as metal and metal oxide particles, can easily be collected and recycled [17]. In addition to this advantage, this surface treatment process is inexpensive [18].

However, previous researchers mostly focused on metallic specimens with flat surfaces. The current work reports a novel configuration of the piezoelectric transducer, which is designed as a type of the combination of rod and ring. Utilizing this kind of transducer, the efficiency for peening cylindrical workpieces can be increased compared to the experiments using longitudinal vibration transducer. In this paper, the simulations of the new transducer and the sound field are first described. Then, the results of experiments on the cavitation field and the peening process are shown.

2. The Novel Transducer

A novel configuration of the piezoelectric transducer was designed and manufactured at the Institute of Dynamics and Vibration Research (Leibniz University Hannover, Germany). The transducer consisted of one set of piezoelectric elements, an Al alloy cover part, a horn part, and a ring sonotrode. The ring sonotrode was made of Al alloy and the diameter of inner ring was 21.5 mm. The PZT (lead zirconate titanate ceramic) plates were assembled between the cover and the horn to excite longitudinal vibration, achieving the elliptical vibration of the ring sonotrode. The harmonic simulation result is shown in Figure 1. The resonance frequency of the transducer was about 21,034 Hz. Low-frequency ultrasound, such as 21 kHz, can introduce more violent cavitation at the same vibration amplitude compared to high-frequency ultrasound. The reason is that at low-frequency ultrasound, the bubble growth period becomes longer, resulting in higher bubble energy

accumulation. As shown in Figure 1, when the ring sonotrode vibrates, there are four small areas with high vibration amplitude, which leads to the generation of stronger cavitation near the four areas. Thus, there are four areas of the workpiece surface that can be peened when they are put into the center of the ring sonotrode. In this way, the efficiency of the ultrasonic cavitation peening for cylindrical workpieces is improved four times over the traditional longitudinal vibration transducer.

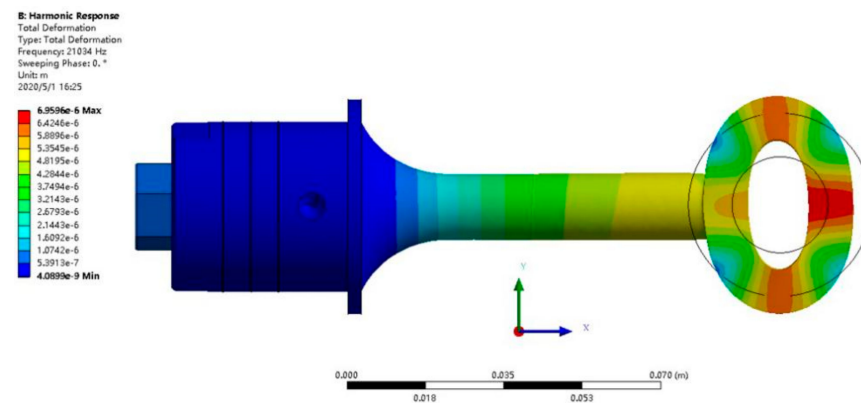


Figure 1. The harmonic simulation result at about 21 kHz.

In order to verify the real vibration shape and resonance frequency of the ring sonotrode, we built a measurement setup using a 3D Laser Doppler vibrometer (MSA-100-3D, Ploytec Company, Waldbronn, Germany). The laser head of the vibrometer can move in the Z direction and the XY positioning stage can achieve the two-dimensional motion in the horizontal plane. The transducer was placed on two support blocks to make the plane of circular ring horizontal, and then they were fixed on a XY positioning stage for obtaining vibration characteristics of all points on the vibrating system. The number of the points on the edge of the ring was set to 80. During the experimentations, the Langevin transducer and the circular ring were tested with the excitation signals of 1 V. As shown in Figure 2, the resonance frequency was 21,025 Hz, which is very close to the simulation results. It also can be seen that the vibration amplitude of the ring sonotrode in the x direction was almost the same as that in the y direction. At the resonance frequency, a relationship of approximately $0.012 \mu\text{m}/\text{V}$ existed between the vibration amplitude and the driving voltage in the range of 0 V and 400 V according to the measurements.

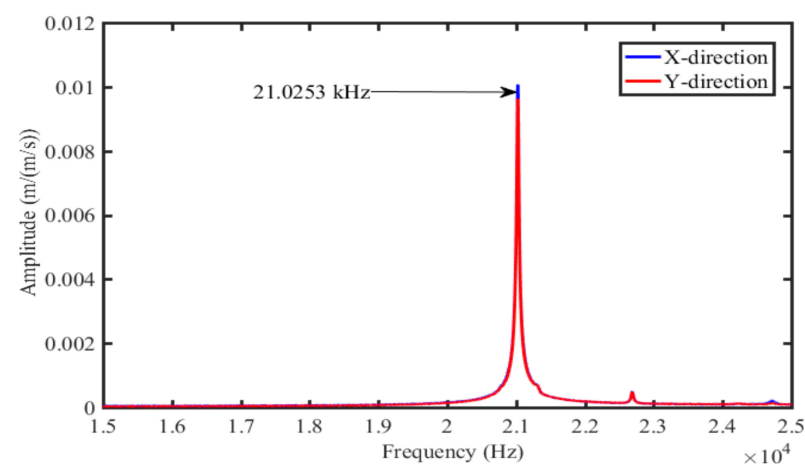


Figure 2. The measured frequency–amplitude curves of the ring sonotrode.

3. Cavitation Experiments

In this part, three different kinds of experiments were carried out to detect cavitation areas, cavitation intensity, and the properties of the peened surfaces. If the metallic rods

are directly treated and then measured, it will be very time-consuming, involving tedious steps. To avoid this, we pasted the aluminum foil around the metallic rod to evaluate the cavitation treatment areas, and then the sonochemiluminescence (SCL) experiments were used to obtain the cavitation intensity. Finally, the surface treatment experiments were carried out to evaluate the surface properties utilizing this novel method. According to previous investigations [19], working distances are very sensitive to the results of the ultrasonic cavitation peening. It is important to study the effects of working distances on the cavitation areas. Hence, the diameters of the metallic rods in these experiments were 13, 14, 15, 16, 17, and 18 mm. The driving voltages were 110, 130, 150, 170, and 190 V. The experimental block scheme is shown in Figure 3.

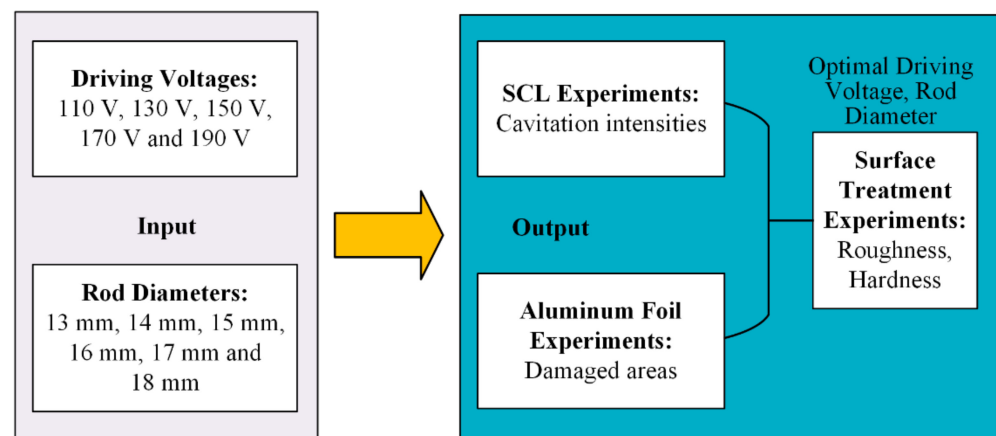


Figure 3. The block scheme for cavitation experiments.

The experimental setup is shown in Figure 4. The function generator (Agilent 33210A, Santa Clara, CA, USA) was used to provide the sinusoidal signals (V_{p-p} : 5 V). A power amplifier (QSC RMX 4050HD, Costa Mesa, CA, USA) was used to amplify the driving voltages, and the oscilloscope (Tektronix DPO 3014, Beaverton, OR, USA) recorded the signals on the transducer. A current probe (Tektronix P6139A, Beaverton, OR, USA) and a voltage probe (Tektronix P5205, Beaverton, OR, USA) were used to measure the output current and voltage, respectively. A tube with a transparent bottom was attached to one side of the ring sonotrode, which can make the inner volume of the sonotrode fill with water. The metallic rod with the aluminum foil was fixed at the center of the sonotrode by a fixture. Each sample was treated for 60 s. Tap water was used and the temperature was 22 ± 1 °C during cavitation experiments. After each treatment, the water was replaced to ensure a small change in in the range of 1 °C. The damaged foils were pasted on a flat plate and then scanned by a microscope (Alicona InfiniteFocus SL-2, Raaba, Austria).

For sonochemiluminescence (SCL) experiments, the experimental solution was made of luminol ($C_8H_7N_3O_2$) (0.004 mol/L), NaOH (0.1 mol/L), and water. SCL is a phenomenon of light emission that is produced by the OH^- and the sonochemically oxidized luminol. Thus, the spatial distribution of cavitation bubbles in an aqueous solution can be indirectly shown by the SCL method. SCL images were captured by the camera (18–250 mm/f3.5–6.3, ISO400, focal length 262 mm) with an exposure time of 90 s. Since the light caused by SCL is weak and cannot be seen by the naked eye, a long exposure time is necessary to obtain a high-quality photo. All of the experiments were carried out in a dark room. Since the sonotrode is cylindrical, the available area of the SCL photo is a circular region.

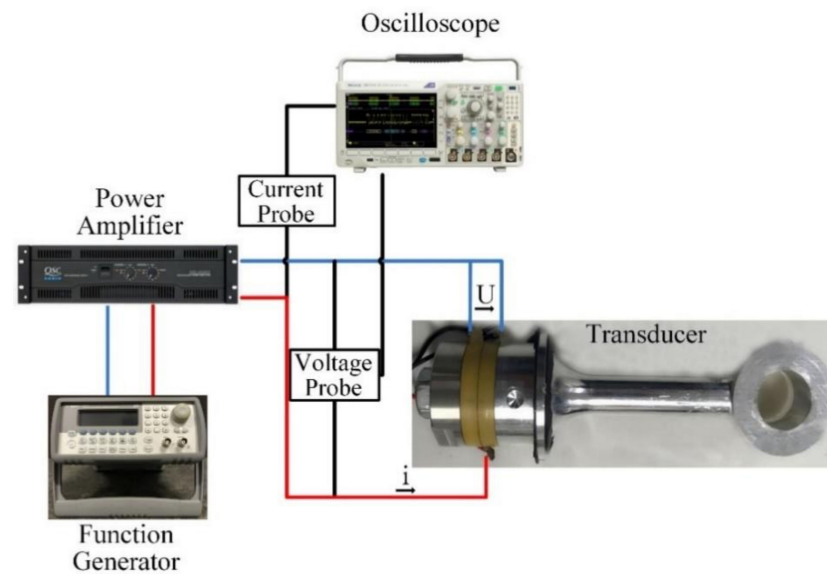


Figure 4. The experimental setup of cavitation processing for cylindrical workpieces.

The cavitation processing time for the cylindrical working pieces was 240 s. For the measurements of the surface properties, we used a hardness tester as per reference [20]. The material of the rod samples was made of Al alloy. The surface roughness was measured by an Alicona microscope. The microscope was used to capture the aluminum foil with a magnification of $5\times$ after treatments.

When the ring sonotrode was filling with water, the damping on the transducer changed, resulting in the changing of resonance frequency. The damping was related to the vapor volume fraction of the water and the tension of water between walls. With different driving voltages, the intensity of cavitation changed due to the change of vibration amplitude of the ring sonotrode. The cavitation intensity was directly related to the vapor volume fraction of the water. Thus, the driving voltage and the working distance affected the resonance frequency of the transducer. The measured resonance frequencies at different experimental conditions are listed in Table 1.

Table 1. The resonant frequencies after filling with water at different conditions.

Diameter (mm)	Voltage (V)					
	110	130	150	170	190	
13	20,650	20,650	20,650	20,670	20,670	
14	20,640	20,640	20,640	20,660	20,660	
15	20,570	20,570	20,570	20,600	20,620	
16	20,540	20,540	20,540	20,560	20,570	
17	20,340	20,340	20,340	20,360	20,360	
18	20,300	20,300	20,300	20,330	20,330	

4. Results

After treating the metallic rods with aluminum foil with 60 s, we observed four separated damaged areas on each foil. The four damaged areas corresponded to the locations of the maximum amplitudes of the ring sonotrode, as shown in Figure 1. After a long period of cavitation processing, the areas where the cavitation bubbles occurred were considered potential damaged areas, which are shown surrounded by red lines in Figure 5. The damaged foil with a diameter of 14 mm at the driving voltage of 190 V is shown as an example in this figure.

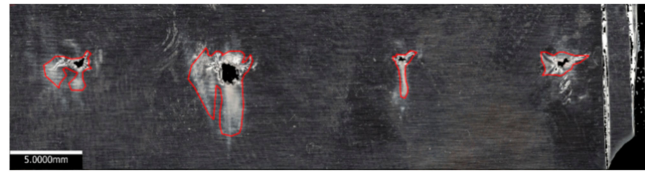


Figure 5. Scanned surfaces of the aluminum foils at the driving voltage of 190 V and at the diameter of 14 mm.

All damaged areas in different experimental conditions are plotted in Figure 6. It can be seen that the increase of the damaged areas corresponded to the increase of the diameter of the rods. At the driving voltage of 110 V, the difference between the maximum and minimum damaged area was about 8 mm², but the difference increased to about 14 mm². Thus, the higher driving voltage caused the larger damaged area. A smaller driving voltage had less effect on the damaged area.

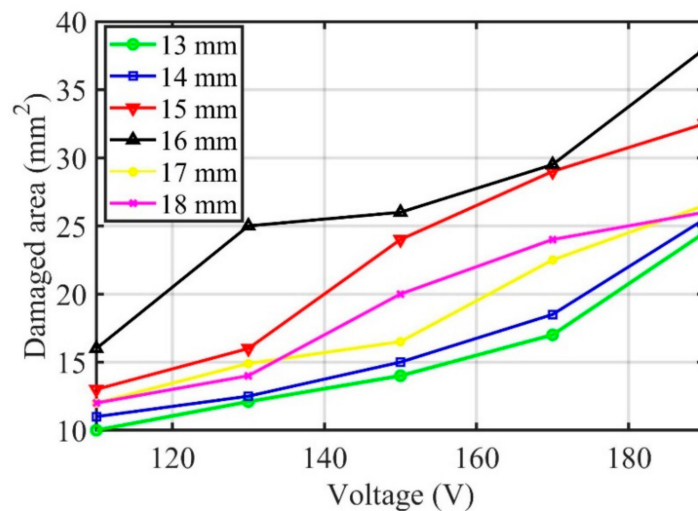


Figure 6. The damaged area of aluminum foils around the metallic rods at different experimental conditions.

After the experiments of the damaged aluminum foils, we carried out the SCL experiments. The intensity of cavitation can be reflected by the relative blue light intensity in the photos of the SCL experiments. Thus, by analyzing the blue light intensity of the photos, we were able to obtain the spatial distribution of the cavitation field. In order to reduce the distraction of other light from the surroundings, we subtracted the relative light intensity by the background light intensity. For every photo, the surrounding light intensities in four different areas beyond the available area were calculated as the average value. Figure 7 shows the distribution of the blue value at the diameter of 13 mm at the driving voltage of 190 V as an example. From this image, it can be clearly seen that there were four areas with strong light intensity, which is similar to the results from the experiments on the damaged aluminum foils. It can also be seen that the light intensity of the four areas was slightly different, which was caused by the differences in the vibration amplitude of the sonotrode and the location of the rod, resulting in the distribution of the sound field during the experiments.

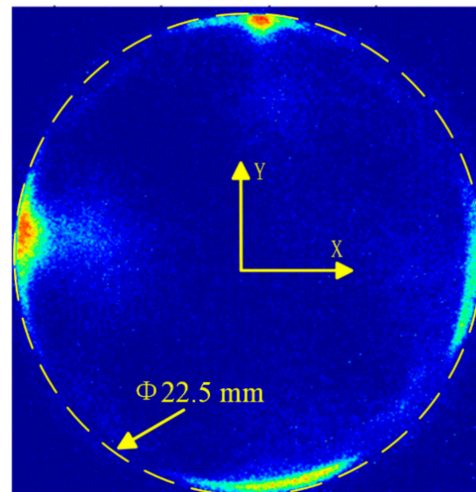


Figure 7. The distribution of the blue value at the diameter of 13 mm at the driving voltage of 190 V.

Figure 8 shows the value of average light intensities for metallic rods with different diameters. The impedance of the transducer was about 95Ω during cavitation processing. Thus, the powers were 127, 178, 237, 304, and 380 W at the driving voltages of 110, 130, 150, 170, and 190 V, respectively.

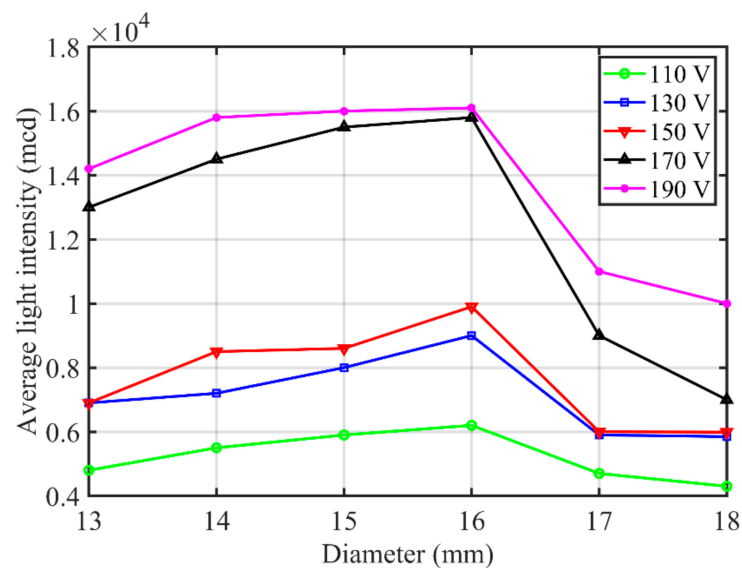


Figure 8. The average light intensities with metallic rods at different conditions.

From the experiments described, we can confirm that the condition of the diameter of 16 mm and the driving voltage of 190 V was optimal in our experimental conditions. One of the ultrasonic cavitation peening experiments was carried out in this case. The other one was carried out at a diameter of 15 mm in order to have a reference. Before the experiments, the surfaces were polished, and the surface roughness was as low as $0.1 \mu\text{m}$. For each of the experiments, six workpieces were treated for 240 s. After treatment, surface roughness was measured in four areas, with five points randomly selected in each area, and then all the measured values were averaged. The results are shown in Table 2. It can be seen that the value of the surface roughness increased to about $2.2 \mu\text{m}$, but the roughness in the two types of experiments showed little difference. It was deduced that the change in diameter had less effect on the surface roughness after treatments.

Table 2. The average surface roughness after ultrasonic cavitation peening.

Diameter	Average R_a (μm)
15 mm	2.24 ± 0.56
16 mm	2.86 ± 0.68

The hardness of the samples after treatment was measured as well. Surface hardness was measured in four areas, with five points randomly selected in each area, and then all the measured values were averaged. The average values are shown in Table 3. The original hardness was about HV 41. After treatment, the hardness increased to HV 50 and HV 56 at the diameters of 15 and 16 mm, respectively. The hardness with the diameter of 16 mm increased by about 36%. Compared to the measured roughness, the hardness obviously changed in the two kinds of experiments. This was due to the advantage of the ultrasonic cavitation peening.

Table 3. The micro hardness of the surface rods before and after cavitation peening.

Diameter	Original Micro Hardness (HV)	Average Micro Hardness (HV)
15 mm	40.05 ± 2.56	50.43 ± 3.53
16 mm	41.45 ± 2.68	56.46 ± 4.32

5. Discussion

From the aluminum foil experiments, it can be seen that the higher driving voltage caused the larger damaged area. The reason was that the higher driving voltage resulted in a higher output power, leading to the generation of more cavitation bubbles on the inner wall of the ring sonotrode. Meanwhile, more cavitation bubbles were generated on the surface of the metallic rod. On the other side, between the driving voltages of 150 and 190 V, the damaged area increased first to a threshold and then decreased. The maximum damaged area corresponding to the diameter of 16 mm was obviously larger than that at other diameters. At the diameter of 16 mm, the gap between the ring sonotrode and the metallic rod was 2.75 mm. At this gap, most of the cavitation bubbles were generated on the rod surface, even at different driving voltages. At large gaps (smaller rod diameter), although the number of the generated cavitation bubbles were the same as the gap of 2.75 mm, the number of the available cavitation bubbles on the rod surface was smaller. This was because the attenuation of the sound pressure increased due to the bubble liquid and there was not enough sound pressure to generate more cavitation bubbles on the surfaces of the rods. At a larger rod diameter, the small gaps limited the dynamics of cavitation bubbles, leading to the change of impacts on the treated surfaces compared to the collapse of bubbles without limitation. When the gap became smaller, the cavitation bubble was no longer spherical if other operation conditions were not changed. Due to this limitation, the impact amplitude on the treated surfaces was reduced.

The average light intensity increased with the increase of the driving voltage, since more power caused more violent cavitation intensity. The strongest light intensity occurred at a diameter of 16 mm. Similar to the descriptions in the experiments of damaged aluminum foils, at the optimal working gap, there was a boundary point between the attenuation of the sound pressure and the limitation of the bubble growth and collapse. Hence, for this novel ultrasonic cavitation peening process, the working gap of about 2.75 mm can be said to be optimal for the treatment of the cylindrical workpieces. Thus, the rod diameter of 16 mm and the driving voltage of 190 V were selected as a set of optimal parameters for the cavitation processing. After treatments, the hardness with the diameter of 16 mm increased by about 36% without significant increase of the surface roughness. From previous investigations [13,14], we can deduce that the residual compressive increased as well.

6. Conclusions

In this paper, the surface enhancement effects of ultrasonic cavitation peening on cylindrical workpieces were investigated utilizing a novel configuration of the piezoelectric transducer with a ring sonotrode. The transducer was designed with a resonance frequency of about 21 kHz and the measured results met the expectation. Since the working gap and the driving voltage play an important role in the properties of the cylindrical workpieces after ultrasonic cavitation peening, we carried out three different kinds of experiments in order to detect cavitation areas, cavitation intensity, and the properties of the peened surfaces. Utilizing the aluminum foil method, we evaluated the cavitation areas on the surfaces of the cylindrical workpieces. The results show that the working gap of 2.75 mm and the driving voltage of 190 V created the largest damaged area on the aluminum foils. In the same case, the SCL experiments showed that the strongest cavitation occurred on the surfaces of the cylindrical workpieces as well. Subsequently, the workpieces were treated in the same condition. After treatment, the surface hardness increased by about 36% without significant increase of the surface roughness. In the previous investigations using the longitudinal transducers [14,20], the hardness increased by about 32% and 44%, respectively. Thus, this novel method has the same effect as a longitudinal transducer and shows potential to improve the efficiency of ultrasonic cavitation peening.

Author Contributions: Conceptualization, F.B. and L.W.; methodology, F.B.; software, G.Q.; validation, K.Y., Z.H. and J.T.; formal analysis, F.B.; investigation, F.B. and G.Q.; resources, G.Q.; data curation, G.Q.; writing—original draft preparation, F.B.; writing—review and editing, F.B. and J.T.; visualization, K.Y.; supervision, J.T.; project administration, L.W.; funding acquisition, Z.H. All authors have read and agreed to the published version of the manuscript.

Funding: This research was supported by the National Natural Science Foundation of China under grant 11974284, and the Fundamental Research Funds for the Central Universities under grants 3102019HHZY03003 and 3102019HHZY030017.

Informed Consent Statement: Informed consent was obtained from all subjects involved in the study.

Data Availability Statement: All data generated or analyzed during this study are included in this article.

Conflicts of Interest: The authors declare no conflict of interest. The funders had no role in the design of the study; in the collection, analyses, or interpretation of data; in the writing of the manuscript; or in the decision to publish the results.

References

1. Zhang, J.; Qiu, Y.; Duan, X.; Yang, C. Precise on-line non-target pose measurement for cylindrical components based on laser scanning. *Assem. Autom.* **2019**, *39*, 596–606. [[CrossRef](#)]
2. Yang, F.; Chen, T.; Lu, Y. The effects of carburization on the fatigue crack growth behaviors of local surface cracks in cylindrical bars. *J. Mater. Eng. Perform.* **2019**, *28*, 3423–3429. [[CrossRef](#)]
3. Bagheri, S.; Mario, G. Review of shot peening processes to obtain nanocrystalline surfaces in metal alloys. *Surf. Eng.* **2009**, *25*, 3–14. [[CrossRef](#)]
4. Unal, O.; Maleki, E.; Varol, R. Effect of severe shot peening and ultra-low temperature plasma nitriding on Ti-6Al-4V alloy. *Vacuum* **2018**, *150*, 69–78. [[CrossRef](#)]
5. Sakamoto, J.; Lee, Y.; Cheong, S. Effect of shot peening coverage on fatigue limit in round bar of annealed medium carbon steel. *J. Mech. Sci. Technol.* **2014**, *28*, 3555–3560. [[CrossRef](#)]
6. Yildirim, H.C.; Marquis, G.B. Fatigue strength improvement factors for high strength steel welded joints treated by high frequency mechanical impact. *Int. J. Fatigue* **2012**, *44*, 168–176. [[CrossRef](#)]
7. Cao, X.; Pian, Y.; Jin, J.; Xu, L.; Wang, C.; Wang, Q. Effects of ultrasonic impact modification on tension-compression fatigue behavior of TC4. *Chin. Surf. Eng.* **2017**, *30*, 48–55.
8. Mordyuk, B.N.; Prokopenko, G.I. Ultrasonic impact peening for the surface properties' management. *J. Sound Vib.* **2007**, *308*, 855–866. [[CrossRef](#)]
9. Takakuwa, O.; Takeo, F.; Sato, M.; Soyama, H. Using cavitation peening to enhance the fatigue strength of duralumin plate containing a hole with rounded edges. *Surf. Coat. Technol.* **2016**, *307*, 200–205. [[CrossRef](#)]
10. Takakuwa, O.; Gill, A.S.; Ramakrishnan, G.; Mannava, S.R.; Vasudevan, V.K.; Soyama, H. Introduction of compressive residual stress by means of cavitation peening into a titanium alloy rod used for spinal implants. *Mater. Sci. Appl.* **2013**, *4*, 23–28. [[CrossRef](#)]

11. Zhao, F.; Bernstein, W.Z.; Naik, G.; Cheng, G.J. Environmental assessment of laser assisted manufacturing: Case studies on laser shock peening and laser assisted turning. *J. Clean. Prod.* **2010**, *18*, 1311–1319. [[CrossRef](#)]
12. Yang, C.; Hodgson, P.D.; Liu, Q.; Ye, L. Geometrical effects on residual stresses in 7050-T7451 aluminum alloy rods subject to laser shock peening. *J. Mater. Process. Technol.* **2008**, *201*, 303–309. [[CrossRef](#)]
13. Sriraman, M.R.; Vasudevan, R. Influence of ultrasonic cavitation on surface residual stresses in AISI 304 stainless steel. *J. Mater. Sci.* **1998**, *33*, 2899–2904. [[CrossRef](#)]
14. Gao, Y.; Wu, B.; Liu, Z.; Zhou, Y.; Shen, N.; Ding, H. Ultrasonic cavitation peening of stainless steel and nickel alloy. *J. Manuf. Sci. E-T ASME* **2014**, *136*, 014502. [[CrossRef](#)]
15. Bai, F.; Wang, L.; Saalbach, K.A.; Twiefel, J. A novel ultrasonic cavitation peening approach assisted by water jet. *Appl. Sci.* **2018**, *8*, 2218. [[CrossRef](#)]
16. Bai, F.; Saalbach, K.A.; Long, Y.; Twiefel, J.; Wallaschek, J. Capability evaluation of ultrasonic cavitation peening at different standoff distances. *Ultrasonics* **2018**, *84*, 38–44. [[CrossRef](#)] [[PubMed](#)]
17. Shchukin, D.G.; Skorb, E.; Belova, V.; Mohwald, H. Ultrasonic cavitation at solid surfaces. *Adv. Mater.* **2011**, *23*, 1922–1934. [[CrossRef](#)] [[PubMed](#)]
18. Bai, F.; Saalbach, K.; Twiefel, J.; Wallaschek, J. Effect of different standoff distance and driving current on transducer during ultrasonic cavitation peening. *Sens. Actuator A Phys.* **2017**, *261*, 274–279. [[CrossRef](#)]
19. Bai, F.; Long, Y.; Saalbach, K.A.; Twiefel, J. Theoretical and experimental investigations of ultrasonic sound fields in thin bubbly liquid layers for ultrasonic cavitation peening. *Ultrasonics* **2019**, *93*, 130–138. [[CrossRef](#)]
20. Bai, F.; Saalbach, K.A.; Wang, L.; Wang, X.; Twiefel, J. Impact of time on ultrasonic cavitation peening via detection of surface plastic deformation. *Ultrasonics* **2018**, *84*, 350–355. [[CrossRef](#)] [[PubMed](#)]